ChemComm

Accepted Manuscript

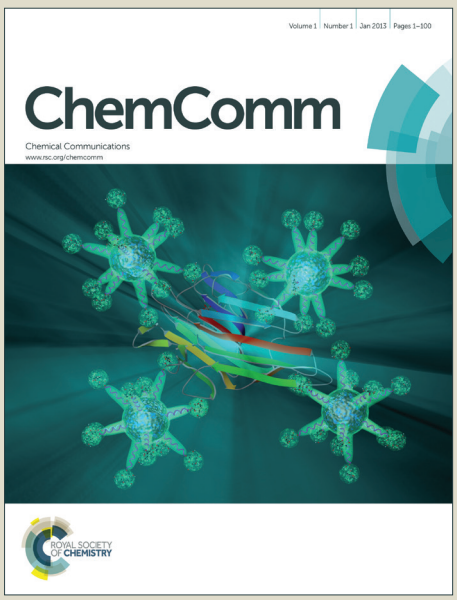

ROYAL SOCIETY OF CHEMISTRY

www.rsc.org/chemcomm

Cite this: DOI: 10.1039/c0xx00000x

www.rsc.org/xxxxxx

COMMUNICATION

Detection of cancer cells using triplex DNA molecular beacons based on expression of enhanced green fluorescent protein (eGFP)

Dongmei Xi,[a] Xindong Wang,[b] Shiyun Ai[b] and Shusheng Zhang[a] *

Received (in XXX, XXX) Xth XXXXXXXXX 20XX, Accepted Xth XXXXXXXXX 20XX

DOI: 10.1039/b000000x

A novel strategy was proposed for Ramos cell detection by combining the expression of enhanced green fluorescent protein (eGFP) with the cell aptamer recognition and the triplex molecular beacons. This system was successfully applied to cancer cell detection with high sensitivity and specificity.

Accurate diagnosis of cancer at its earliest stages is the key to improve the cure rate and decrease the therapy costs.[1] It has been demonstrated that cancer originating from genetic abnormalities can usually cause the affected cells to behave abnormally at the molecular level.[2,3] Most previous studies for cancer diagnosis have relied on the histopathological and morphological observation of tumor tissues.[4,5] However, those methods have significant limitations that may confound clinical data analysis and mislead diagnosis. Therefore, development of a method for sensitive and selective detection of cancer cells is of great significance for early diagnosis and treatment of cancer.

Currently, imaging has become an advanced and versatile tool for cancer research.[6] So far, various imaging technologies have been developed, among which total internal reflection fluorescence microscopy (TIRFM) is a powerful tool for observing the distribution and movement of fluorescent molecules in an aqueous environment.[7] This highly sensitive technique can be used when the molecules of interest are very close to the boundary between the aqueous environment and another medium with a higher refractive index.[8] TIRFM provides a higher spatial resolution and a higher signal-to-noise ratio than classic fluorescence microscopy or laser scanning confocal microscopy.[9] Because TIRFM is unparalleled in its imaging capability in the near-boundary field, it has been successfully applied to *in vivo* studies of cells for the past decade,[10] and is believed to play increasing roles in early cancer diagnosis.

[a] *Shandong Province Key Laboratory of Detection Technology for Tumor Makers, College of Chemistry and Chemical Engineering, Linyi University, Linyi 276005, P. R. China. E-mail: shushzhang@126.com; Fax: +86-539-8766867; Tel: +86-539-8766867.*

[b] *College of Chemistry and Material Science, Shandong Agricultural University, Taian 271018, P. R. China.*

† Electronic Supplementary Information (ESI) available: Experimental procedures and additional figures. See DOI: 10.1039/c000000x/

Nowadays, the rapid development of genetic engineering has brought revolutionary changes in the medicine. Genetic engineering, also known as recombinant DNA technology, is the collection of a wide array of techniques that alter the genetic constitution of cells or individuals by selective removal, insertion, or modification of individual genes or gene sets.[11] Recombinant DNA is a hybrid DNA molecule created in the test tube by joining a DNA fragment of interest with a carrier DNA.[12] The recombinant DNA can be expressed in host organism. During this process, the gene is transcribed into mRNA and mRNA is translated into proteins. By cultivating host organism, large quantities of the gene products can be harvested and purified. Currently, genetic engineering holds tremendous promise for medicine and human well-being.[13] Medical applications of genetic engineering include diagnosis for genetic and other diseases, treatment for genetic disorders, production of safer and more effective vaccines and pharmaceuticals, and so on.[14] Owing to the tremendous potentiality of the recombinant DNA technology, it may be a powerful technique in bioanalytical applications and cancer diagnosis.

Based on that, a novel method for the detection of Ramos cells (human Burkitt's lymphoma cells) was presented by combining the expression of eGFP protein with the cell aptamer recognition and the triplex molecular beacons. Scheme 1 depicts the assay protocol. DNA aptamers for Ramos cells were first immobilized on the surface of magnetic Fe_3O_4–Au core–shell nanoparticles (Fe_3O_4@Au), and then hybridized partly with its complementary DNA sequence (cDNA). Upon the addition of a covalently closed circular duplex DNA, named as plasmid, the cDNA has the correct sequence to form a triplex with the plasmid in the presence of a triplex DNA binder. When the Ramos cells were introduced, the aptamers could bind to the cells and formed Fe_3O_4@Au-DNA/target complexes, resulting in the release of the triplex structures. Subsequently, the triplex DNA structures were transformed into a cell-free protein synthesis system. In this system, transcription initiation, elongation, and termination of the eGFP gene cloned in the plasmid was triggered successively, leading to the production of mRNA molecules. Then the translation of the eGFP occurred under the direction of mRNA, the process of which included three coordinated stages: initiation, elongation, and termination. As a result, high levels of eGFP proteins were produced. Quantitative analysis was performed by reading the fluorescence intensity of the eGFP, and imaging was

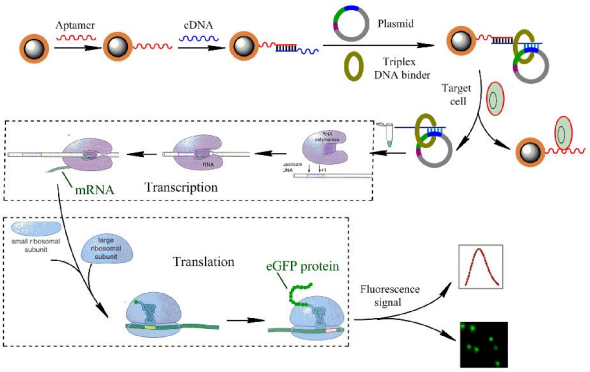

Scheme 1 Schematic illustration of the cancer cell detection through aptamer recognition and expression of the eGFP.

realized through TIRFM.

The assay was based on a newly constructed vector pEHISEGFPTEV-M. To construct pEHISEGFPTEV-M, plasmid pEHISEGFPTEV was digested with restriction enzymes BamHI/HindIII and the digested plasmid was isolated. Two DNA strands complementary to each other were synthesized and hybridized to form the double-stranded DNA. The duplex DNA was then ligated into the digested vector. The diagram of the resulting new plasmid pEHISEGFPTEV-M is shown in Fig. 1A. To confirm its integrity, pEHISEGFPTEV-M was digested by BamHI/HindIII and then analyzed by 1.0% agarose gel electrophoresis, as shown in Fig. 1B. The new plasmid contains a T7 promoter and eGFP coding sequence, and thus is able to express eGFP proteins using the expression system in the downstream step.

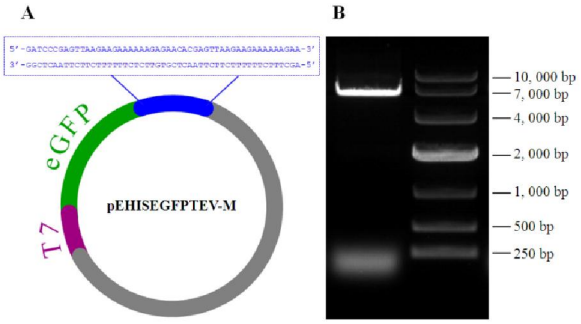

Fig. 1 (A) Diagram of plasmid pEHISEGFPTEV-M. Sequences within the dashed box are inserted into the plasmid and will form a triplex with the cDNA. (B) Restriction endonuclease pattern of plasmid pEHISEGFPTEV-M. The plasmid pEHISEGFPTEV-M was digested with BamHI/HindIII, and analyzed by 1.0% agarose gel electrophoresis.

To evaluate the feasibility of this assay, the plasmid pEHISEGFPTEV-M was firstly expressed in protein expression system. To shorten the reaction time and improve the product levels, S30 T7 high yield protein expression system was employed. This system simplifies the transcription and translation of the eGFP cloned in plasmid by providing an extract that contains T7 RNA polymerase for transcription and all necessary components for translation. The plasmid was quantified by determining the expression levels of eGFP monitored by the fluorescence intensity (excitation maximum = 488 nm, emission maximum = 509 nm). Under the optimal conditions, the dynamic range of the designed method for plasmid detection was examined. As shown in Fig. S1A, the fluorescence signal was easily observed to increase with the increase in plasmid concentration, and reached a maximum at 500 pM. A linear dependence between the peak fluorescence and the DNA concentration was obtained in the range of 0 to 500 pM as shown in Fig. S1B. The regression equation could be expressed as y (a. u.) = 3.1204 x (pM) + 210.4015 (R = 0.9963). But introduction of the DNA at higher concentrations (> 500 pM) decreased the intensity (Fig. S1C, ESI). This might be attributed to the increase in the incidence of internal translational initiation or the number of prematurely arrested translation products caused by an increased amount of DNA. In this study, detection of the cancer cells was realized through the expression of the eGFP cloned in the plasmid. Satisfactorily, the data confirmed the feasibility of the strategy.

One of the most important factors affecting the sensitivity of the assay is the levels of the eGFP protein synthesized, which are closely related to the transcription/translation time. Quantitative detection of Ramos cells was realized by determining the expression levels of eGFP protein. The change in the fluorescence signal of eGFP with reaction time was investigated. As shown in Fig. S2 (ESI), the fluorescence intensity was observed to increase gradually with the increase in time from 0.5 h to 1.5 h, followed by a decrease in 2 h. Just to meet the requirement of fast reaction and sensitivity in analytical work, the reaction time of 1 h was selected for the following experiments.

Quantitative detection of Ramos cells was performed under optimum conditions. As shown in Fig. 2A, the intensities of the fluorescence emission of the eGFP protein at 509 nm intensified with the increase in target cell amounts. Moreover, the values of fluorescence intensities had a linear dependence on the logarithmic number of Ramos cells in a wide range from 500 to 10^6 cells mL^{-1} (Fig. 2B). The regression equation could be expressed as y (a. u.) = 403.8451 log cells mL^{-1} – 864.3792 (R = 0.9875). The limit of detection (LOD) was calculated to be 398 Ramos cells by using 3σ. A series of three measurements of 2000 Ramos cells mL^{-1} yielded a reproducible signal with a relative standard deviation (RSD) of 7.9%. The sensitivity of the assay is comparable or more sensitive than those of the most reported methods,[15] and the details are shown in Table S2 (ESI). The high sensitivity could be attributed to not only the specific recognition between aptamers and targets on the cell surface, but also the high-level expression of the eGFP in the protein synthesis system. Notably, A DNA diagnostic system was developed in previous reports,[16] in which *E. coli* was incorporated

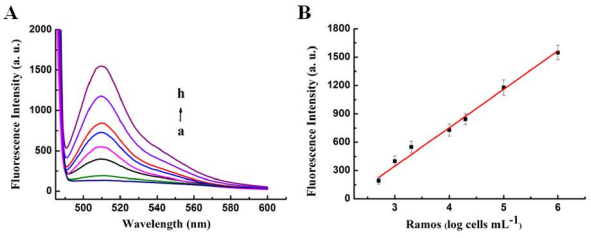

Fig. 2 (A) Relationship between the eGFP fluorescence intensities and the concentrations of the Ramos cells. From a to h: 0, 500, 10^3, 2 × 10^3, 10^4, 2 × 10^4, 10^5, 10^6 cells mL^{-1}. (B) The linear relationship between the fluorescence intensities and logarithmic concentration of Ramos cells. The error bars are standard deviations of three repetitive measurements.

as a reported probe and 7-57 hours were needed for the test. In the current assay, however, triplex DNA was used as a reporter probe for cell detection, and one hour was enough to meet the sensitivity requirements.

Imaging of the eGFP protein was realized by TIRFM. As the TIRFM technique is unrivaled in its imaging capability in the near-boundary field, it is hoped to visualize the eGFP protein when introducing a small amount of cancer cells. Satisfactorily, no signal was observed in the absence of Ramos cells (Fig. 3A). When 100 cells mL^{-1} was introduced, specific green fluorescence signals could be visualized (Fig. 3B), and intensified with the increase in cell amounts (Fig. 3C and D). In the presence of 1000 cells mL^{-1} (Fig. 3E), the fluorescence signals seemed to be similar to that in Fig. 3D. In fact, however, introduction of 1000 cells mL^{-1} produced fluorescence in much wider fields of image, indicating higher protein levels. To confirm the green fluorescence was emitted by the eGFP protein, proteinase K was employed to digest the protein in Fig. 3D. As expected, the signals disappeared (Fig. 3F). It is worth mentioning that the triplex binder, coralyne (CORA), played a key role in stabilizing the triplex DNA. When the CORA was added to the assay solution, almost no background signal was observed in the absence of Ramos cells (Fig. S3A, ESI). Without addition of the CORA, however, we could observe the signals (Fig. S3B, ESI). This was mainly ascribed to the unwinding of the DNA triplex.

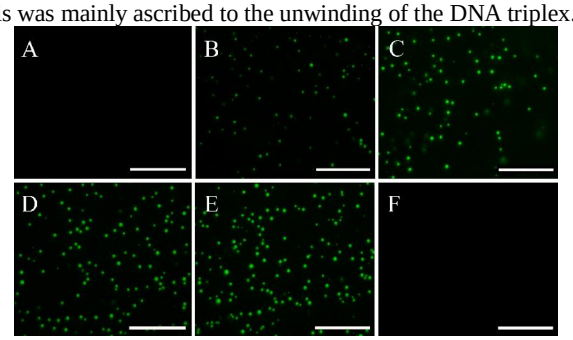

Fig. 3 eGFP fluorescence observations by TIRFM for the detection of Ramos cells at the concentration of (A) 0, (B) 100, (C) 200, (D) 500, (E) 1000 cells mL^{-1}. (F) Fluorescence observation of sample D by TIRFM after digestion with protease K. Scale bar: 25 μm.

To investigate the specificity of this detection system, Ramos cells (target), K-562, MCF-7, Hela, A549 cells, and 0 cells (blank) were detected, respectively. As shown in Fig. S4 (ESI), the eGPF fluorescence signal was only observed in the presence of target cells, while no signal was observed in the absence of Ramos cells or in the presence of the other cells. Thus, the proposed strategy would provide a sensitive and selective platform for qualitative and quantitative detection of cancer cells.

To further evaluate the applicability of the proposed strategy in real biological samples, various amounts of Ramos cells were spiked into normal human serum samples and determined. As shown in Table S3 (ESI), the recovery was found to vary from 90.3% to 95.2%, indicating that the assay has potential application in clinical diagnosis and point-of-care use.

In summary, a novel strategy was developed for Ramos cell detection by combing aptamer recognition and triplex DNA molecular beacons. Significantly, the expression of the eGFP gene was successfully introduced into the analysis system. The transcription and translation of the eGFP was performed in one reaction step in the protein synthesis system and avoided complex operations. Furthermore, the eGFP protein could be quantified directly without introducing any labeled molecule, thereby reducing the background noise. In comparison with the previously reported studies, the label free strategy opens a new horizon for quantitative detection of cancer cells, holding great promise for potential applications for *in vivo* imaging.

This work was supported by the National Science Foundation of China (21275086, 21227008), the Promotive Research Fund for Excellent Young and Middle-aged Scientists of Shandong Province (BS2011SW001), the Open Project of State Key Laboratory of Crop Biology (2011KF10), and the Postdoctoral Foundation of Qingdao University of Science and Technology (400-0022607).

We thank Professor Huanting Liu (the University of St Andrews) for providing the plasmid pEHISEGFPTEV.

Notes and references

1 (a) R. Siegel, D. Naishadham and A. Jemal, *Ca–CancerJ.Clin*., 2012, **62**, 10; (b) Z. Zhang, Q. Luo, X. Yan, Z. Li, Y. Luo, L. Yang, B. Zhang, H. Chen and Q. Wang, *Anal. Chem*., 2012, **84**, 8946.

2 (a) D. Shangguan, Y. Li, Z. Tang, Z. C. Cao, H. W. Chen, P. Mallikaratchy, K. Sefah, C. J. Yang and W. Tan, *Proc. Natl. Acad. Sci. U.S.A.*, 2006, **103**, 11838; (b) A. Llevot and D. Astruc, *Chem. Soc. Rev*., 2012, **41**, 242.

3 S. Bi, B. Ji, Z. P. Zhang and S. S. Zhang, *Chem. Commun*., 2013, **49**, 3452.

4 (a) S. V. Bachawal, K. C. Jensen, A. M. Lutz, S. S. Gambhir, F. Tranquart, L. Tian and J. K. Willmann, *Cancer. Res*., 2013, **73**, 1689; (b) F. A. Greco, K. Oien, M. Erlander, R. Osborne, G. Varadhachary, J. Bridgewater, D. Cohen and H. Wasan, *Ann. Oncol*., 2012, **23**, 298.

5 (a) B. J. Vakoc, D. Fukumura, R. K. Jain and B. E. Bouma, *Nat. Rev. Cancer*., 2012, **12**, 363; (b) M. Perfézou, A. Turner and A. Merkoçi, *Chem. Soc. Rev.*, 2012, **41**, 2606.

6 (a) R. Qian, L. Ding and H. Ju, *J. Am. Chem. Soc*,. 2013, **135**, 13282; (b) E. Sharon, E. Golub, A. Niazov-Elkan, D. Balogh and I. Willner, *Anal. Chem.*, **2014**, *86*, 3153; (c) A. R. Yadav, C. R. Mace and B. L.Miller, *Anal. Chem.*, 2014, **86**, 1067.

7 Y. Wan, W. M. Ash, L. Fan, H. Hao, M. K. Kim and J. Lin, *Plant. Methods.*, 2011, **7**, 27.

8 H. Tanaka, S. Fujii and T. Hirano, *Nat. Protoc.*, 2014, **9**, 76.

9 (a) J. T. Groves, R. Parthasarathy and M. B. Forstner, *Annu. Rev. Biomed. Eng.*, 2008, **10**, 311; (b) R. Yokokawa, Y. Kitazawa, K. Terao, A. Okonogi, I. Kanno and H. Kotera, *Biomed. Microdevices.*, 2012, **14**, 791.

10 B. D. Khalil, S. Hanna., B. A. Saykali, S. El-Sitt, A. Nasrallah, D. Marston, M. El-Sabban, K. M. Hahn, M. Symons and M. El-Sibai, *Exp. Cell. Res*., 2014, **321**, 109.

11 V. Meyer, *Biotechnol. Adv*., 2008, **26**, 177.

12 R. J. Grant-Klein, L. A. Altamura and C. S. Schmaljohn, *Virus. Res*., 2011, **162**, 148.

13 (a) I. M. Verma, *Science*, 2013, **341**, 853; (b) Z. Garate, B. R. Davis, O. Q. Bustamante and J. C. Segovia, *Hum. Gene. Ther*., 2013, **24**, 571.

14 J. Polak and L. Hench, *Gene. Ther*., 2005, **12**, 1725.

15 (a) J. E. Smith, C. D. Medley, Z. Tang, D. Shuangguan, C. Lofton and W. Tan, *Anal. Chem.*, 2007, **79**, 3075; (b) Q. Shen, L. Xu, L. Zhao, D. Wu, Y. Fan, Y. Zhou, W. H. Ouyang, X. Xu, Z. Zhang, M. Song, T. Lee, M. A. Garcia, B. Xiong, S. Hou, H. R. Tseng and X. Fang, *Adv. Mater.*, 2013, **25**, 2368; (c) G. Liu, X. Mao, J. A. Phillips, H. Xu, W. Tan and L. Zeng, *Anal. Chem.*, 2009, **81**, 10013; (d) J. Zhao, L. Zhang, C. Chen, J. Jiang and R. Yu, *Anal. Chim. Acta*, 2012, **745**, 106; (e) T. Deng, J. Li, L. L. Zhang, J. N. Chen, G. L. Shen and R.Q. Yu, *Biosens. Bioelectron.*, 2010, **25**, 1587.

16 Y. Yan, W. Sha, J. Sun, X. Shu, S. Sun and J. Zhu, *Chem. Commun*., 2011, **47**, 7470.